HAL
open science

Âge K/Ar et contrôle structural de mise en place des veines épithermales à Au-Ag de la Cordillera Shila, Sud Pérou.

Daniel Cassard, Alain Chauvet, Laurent Bailly, Fernando Llosa, Juan Rosas, Eric Marcoux, Catherine Lerouge

To cite this version:

Daniel Cassard, Alain Chauvet, Laurent Bailly, Fernando Llosa, Juan Rosas, et al.. Âge K/Ar et contrôle structural de mise en place des veines épithermales à Au-Ag de la Cordillera Shila, Sud Pérou.. Comptes rendus de l'Académie des sciences. Série IIa, Sciences de la terre et des planètes, 2000, 330, pp.23-30. 10.1016/S1251-8050(00)00118-X . hal-00093019

HAL Id: hal-00093019

https://insu.hal.science/hal-00093019v1

Submitted on 5 Mar 2013

HAL is a multi-disciplinary open access archive for the deposit and dissemination of scientific research documents, whether they are published or not. The documents may come from teaching and research institutions in France or abroad, or from public or private research centers.

L'archive ouverte pluridisciplinaire **HAL**, est destinée au dépôt et à la diffusion de documents scientifiques de niveau recherche, publiés ou non, émanant des établissements d'enseignement et de recherche français ou étrangers, des laboratoires publics ou privés.

C. R. Acad. Sci. Paris, Sciences de la Terre et des planètes / Earth and Planetary Sciences 330 (2000) 23–30
© 2000 Académie des sciences / Éditions scientifiques et médicales Elsevier SAS. Tous droits réservés
S125180500000118X/FLA

Geomaterials / Géomatériaux

Structural control and K/Ar dating of the Au–Ag epithermal veins in the Shila Cordillera, southern Peru

Daniel Cassard[a]*, Alain Chauvet[b], Laurent Bailly[a], Fernando Llosa[c], Juan Rosas[c], Eric Marcoux[b], Catherine Lerouge[a]

[a]BRGM, DR/LGM, BP 6009, 45060 Orléans cedex 2, France
[b]CNRS–UMR 6530, université d'Orléans, BP 6759, 45067 Orléans cedex 2, France
[c]CEDIMIN S.A., Luis N. Saenz 447–449, Jesus Maria–Lima 21, Peru

Received 3 May 1999; accepted 22 November 1999

Communicated by Zdenek Johan

Abstract — The Au–Ag epithermal mineralization of the Shila Cordillera is dated at about 10.7 Ma (K/Ar on adularia). The vein system is characterized by the association of a major ≈east–west vein and N120–135°E secondary fractures. The strike-slip faults controlling the veins indicate an initial NE–SW to ENE–WSW shortening direction, which is compatible with that generally accepted for this period. These structures were reopened during a second phase and channelized mineralizing fluids, the circulation of which may have began at the end of stage 1. © 2000 Académie des sciences / Éditions scientifiques et médicales Elsevier SAS

Peru / Shila Cordillera / epithermal gold / vein / structural control / K/Ar ages

Résumé — Âge K/Ar et contrôle structural de mise en place des veines épithermales à Au–Ag de la Cordillera Shila, Sud Pérou. Les minéralisations épithermales à Au–Ag de la Cordillera Shila sont datées à environ 10,7 Ma (K/Ar sur adulaire). Le système de veines est caractérisé par l'association entre une veine principale sensiblement est–ouest et des fractures satellites N120 à N135°E. Les décrochements contrôlant les veines indiquent une direction de raccourcissement initiale NE–SW à ENE–WSW, compatible avec celle généralement admise pour cette période. Dans un deuxième stade, ces structures sont ré-ouvertes pour servir de réceptacle aux fluides minéralisateurs, dont la circulation débute probablement dès la fin du stade 1. © 2000 Académie des sciences / Éditions scientifiques et médicales Elsevier SAS

Pérou / Cordillera Shila / or épithermal / veine / contrôle structural / âges K/Ar

1. Introduction

The Arequipa–Orcopampa area (southern Peru), about 600 km to the south-east of Lima, is characterized by several base- and precious-metal epithermal districts (Arcata, Caylloma, Madrigal, Orcopampa, Shila, Suykutambo), hosted by Neogene volcanics (*figure 1*). Few studies have been carried out on the structural control of the mineralization (e.g. [1, 3, 4, 10]), with somewhat contradictory results. The structural context of the Au–Ag mineralization of the Shila Cordillera, coupled with the dating of the mineralizing event, has been considered with the aim of examining how mineralization emplacement fits into the broader geodynamic and metallogenic evolution model for this part of the Andean belt.

2. Geological setting

The Shila low-sulphidation epithermal vein system (e.g., [7]) is located in the western Cordillera, northwest

* Correspondence and reprints: d.cassard@brgm.fr

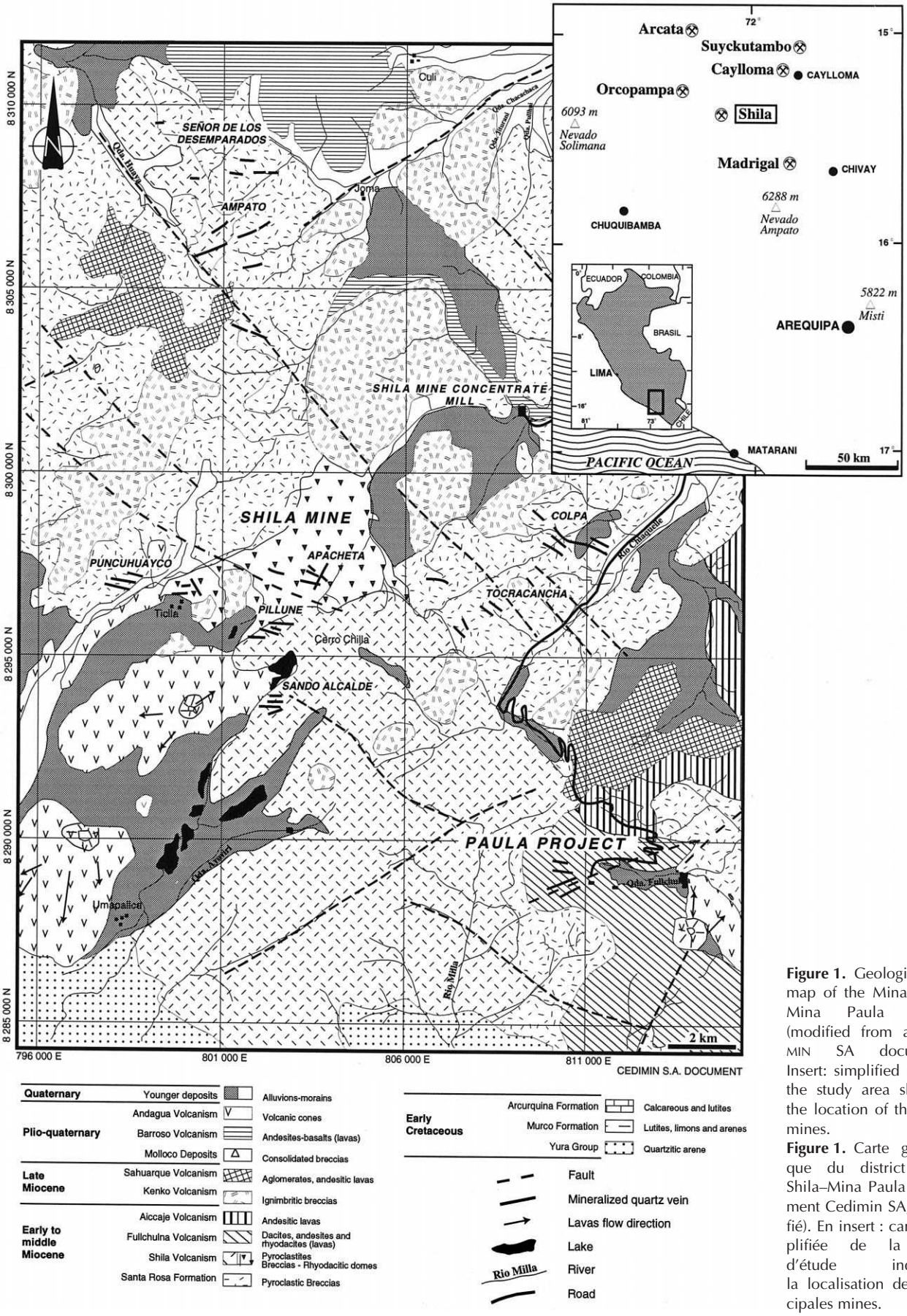

Figure 1. Geological map of the Mina Shila–Mina Paula district (modified from a CEDIMIN SA document). Insert: simplified map of the study area showing the location of the main mines.

Figure 1. Carte géologique du district Mina Shila–Mina Paula (document Cedimin SA, modifié). En insert : carte simplifiée de la zone d'étude indiquant la localisation des principales mines.

Table I. K/Ar age determinations on volcanic rocks from the Shila Cordillera, Pillune area (from [13]).
Tableau I. Âge K/Ar des volcanites de la Cordillera Shila, secteur de Pillune (d'après [13]).

Conventional K/Ar age determinations						
Sample No.	Rock/vein	Material	K_2O (wt.%)	$^{40}Ar \times 10^{-10}$ mol·g^{-1}	^{40}Ar (%)	Age (Ma ± 1σ)
96a	Dacitic flow	whole rock	2.68	0.6044	44.9	13.0 ± 0.6
96b	Dacitic flow	whole rock	2.68	0.5985	57.0	12.9 ± 0.6

of Arequipa. The geology of the area consists of a folded sedimentary basement (sandstone, shale and limestone) of Jurassic (Yura Group) and Cretaceous (Murco and Arcurquina formations) age, unconformably overlain by a complex unit of Neogene volcanic rocks hosting several orebodies (*figure 1*) [14, 23]. The veins are hosted by the Early to Middle Miocene calc-alkaline Shila volcanic breccias and lavas [13].

From 1990 to 1997, the Shila district produced 436 065 metric tons of ore grading 10.2 g·t^{-1} Au and 265.3 g·t^{-1} Ag (CEDIMIN SA, unpublished report). The mineralized veins trend east–west (Pillune, Sando Alcalde, Ticlla, Puncuhuayco, Mina Paula), NW–SE (Apacheta, Colpa, Tocracancha), and exceptionally NE–SW (Apacheta, Puncuhuayca, Ampato) (*figure 1*). The veins are generally thin (0.2 to 2.5 m), steeply dipping (> 75°) to the north or south, and extend horizontally some 100 m for a depth that rarely exceeds 150 m.

3. Mineralogy and hydrothermal alteration

The gangue is composed of quartz–rhodonite/rhodochrosite–adularia. The sulphur-bearing paragenesis is dominated by Ag sulphides and sulphosalts (Ag-tetrahedrite, Ag-tennantite, abundant pearceite, polybasite, jalpaite and acanthite), associated with base metal sulphides (pyrite, sphalerite, chalcopyrite and galena). Most of the electrum is late, deposited at the same time or later than the Ag species.

Two main alteration types are recognized: *i*) potassification of the mesostasis; and *ii*) pseudomorphism of the magmatic biotite and amphibole by a chlorite–epidote–calcite assemblage, associated with partial replacement of the plagioclase phenocrysts and adularia crystals by sericite and calcite.

4. Radiometric dating

New K/Ar ages have been obtained for the host rocks and veins in the district (*tables I* and *II*). Whole rock analyses of the fresh dacite hosting the Pillune vein system yielded two ages of 13.0 ± 0.6 and 12.9 ± 0.6 Ma [13], and analyses of pure adularia from veins of Sando Alcalde and Pillune yielded respective ages of 10.94 ± 0.13 and 10.56 ± 0.12 Ma. Compared to published data on mineralization in the area (*table III*), the Shila mineralization is about 5–7 Ma younger than that of the neighbouring Orcopampa and Caylloma districts and of a similar age to that of the Suyckutambo district.

5. Structural setting

The structural observations made on fracture zones located along the axis of the vetas and on their walls are summarized in the stereogram of *figure 2*. The strike-slip faults controlling the mineralization can be divided into two main groups: (1) a NE–SW- to SE–NW-trending population, showing sinistral kinematics, and (2) an east–west- to SSE–NNW-trending population showing dextral kinematics. The overlapping of the two groups indicates that the structures with similar orientations were affected by different kinematics and demonstrates the existence of several deformation events.

The vein system (*figure 3a*) shows a general pattern characterized by the systematic association of a main vein (N080–110°E; 1–2 m thick) showing complex cockade, brecciated and geodic quartz textures and thin open secondary fractures (N120–135°E) filled with euhedral quartz locally associated with sulphides (*figure 3*). This geometry, which is the most common case, is particularly well represented at Pillune (two main veins), Sando Alcalde and Mina Paula–veta Patricia

Table II. K/Ar age determinations on adularia from veins of the Pillune and Sando Alcalde area (convention E 947, Prof. P.-Y. Gillot).
Tableau II. Âges K/Ar obtenus sur des cristaux d'adulaire des veines des secteurs de Pillune et de Sando Alcalde (convention E 947, prof. P.-Y. Gillot).

Conventional K/Ar age determinations						
Sample no.	Rock / vein	Material	K (%)	$^{40}Ar^*$ (%)	$^{40}Ar^*$ (10^{14}at·g^{-1})	Age (Ma ± 2 σ)
SHP 2	Vein 21	adularia	12.25	51.67	1.36	10.56 ± 0.12
SHS 4	Vein 74	adularia	11.98	53.23	1.37	10.94 ± 0.13

Table III. Age determinations on mineralized and host rock samples from the mining districts of southern Peru.
Tableau III. Âges des minéralisations et des roches encaissantes de différents districts miniers du Sud Pérou.

District	*Rock/vein*	*Material*	*K–Ar age (Ma ± 1σ)*	*$^{40}Ar/^{39}Ar$ age (Ma ± 1 σ)*	*Reference*
	Ag–Au veins	Adularia-wr	17.0 ± 0.5		
	Ag–Au veins	Adularia-v	17.6 ± 0.5 to 17.9 ± 0.5		
Orcopampa	Q-Alunite alteration	Alunite	18.4 ± 0.5 to 19.5 ± 0.6		[5]
District	Sarpane volcanics	Hb / Biot	18.3 ± 0.6 to 19.4 ± 0.6		
	Ag–Au veins	Adularia-wr		17.4 ± 0.4	
	Ag–Au veins	Adularia-v		17.9 ± 0.5	
	Marion vein	Adularia	5.3 ± 0.2		
Arcata	Luisa vein	Adularia	5.5 ± 0.2		[2]
District	Tres Reyes vein	Alunite	5.1 ± 0.3 to 5.4 ± 0.2		
	Tres Reyes vein	Adularia	5.4 ± 0.2 to 5.6 ± 0.2		
	Volcanic host rocks	Glass / biotite	5.9 ± 0.2 to 6.3 ± 0.2		
Caylloma	San Cristobal vein	Adularia-wr	17.1 ± 0.7		[21]
District	San Cristobal vein	Adularia-v	15.8 ± 0.5		
	Bateas vein	Adularia-wr	16.3 ± 0.5		
Suyckutambo District	Ag–Au mineralization	?	11.4 ± 0.4		[17]

wr = wall rock; v = vein

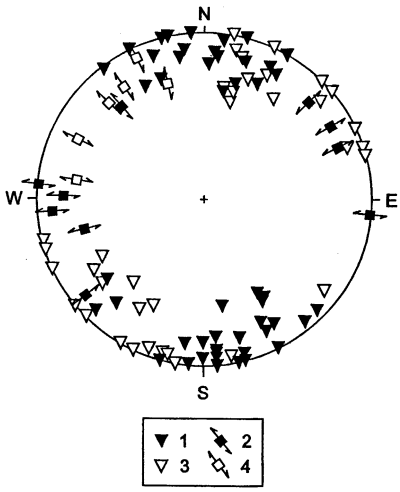

Figure 2. Stereogram of structural data from the veins at Mina Shila (Apacheta, Pillune, Sando Alcalde, Colpa, Tocracancha, Ticlla and Puncuhuayco), Mina Paula, Ampato and Señor de los Desemparados. 95 data points, Schmidt projection, lower hemisphere: 1 = sinistral fault; 2 = sinistral striae; 3 = dextral fault; 4 = dextral striae.

Figure 2. Stéréogramme des données structurales provenant des veines de Mina Shila (Apacheta, Pillune, Sando Alcalde, Colpa, Tocracancha, Ticlla et Puncuhuayco), de Mina Paula, d'Ampato et de Señor de los Desemparados. 95 données, projection de Schmidt, hémisphère inférieur : 1 = faille senestre ; 2 = strie senestre ; 3 = faille dextre ; 4 = strie dextre.

(*figures 3b*, *3h* and *3e*). It is interpreted as resulting from the superimposition of two deformation events. At this high structural level, the first event was characterized by sinistral movement that caused the development of major shear planes (oriented N080–110°E) associated with a crude S1 fracture schistosity, in places sigmoidal (oriented N120–135°E; *figure 3*). Striae are not observed everywhere. The second event reactivated these two types of structure. The major shear planes show evidence of dextral movement and most of the S1 schistosity planes are reopened although some are locally affected by dextral shearing (pull-apart opening). Very locally, the second deformation event caused S2 schistosity (*figures 3c*, *3d* and *3g*). The observed relationships are unequivocal: sinistral-related S1 is systematically cut by dextral-related S2. In other words, the NE–SW to ENE–WSW shortening direction is earlier than the ESE–WNW to SE–NW one.

Figure 3. Examples of the superimposition of deformation events 1 and 2 observed on vein walls. Schistosity 1 is associated with transcurrent deformation corresponding to a NE–SW to ENE–WSW shortening direction. Locally, schistosity 2, also associated with transcurrent deformation, but showing opposed kinematics — i.e. a ESE–WNW to SE–NW shortening direction — is superimposed on schistosity 1 causing its partial obliteration. Reopening of schistosity 1 occurred during this second event. a) Location map of the studied veins from b) Pillune – veta 14, c) Los Desemparados, d) Ticlla, e) veta Patricia, f) Mina Paula, g) Tocracancha – veta Plata, h) Sando Alcalde – veta 74 and i) veta Nazareño.

Figure 3. Exemples de superposition des épisodes de déformation 1 et 2 dans les épontes de quelques « vetas ». La schistosité 1 est associée à une déformation transcurrente, correspondant à une direction de raccourcissement NE–SW à ENE–WSW. Localement, une schistosité 2, également associée à une déformation transcurrente, mais de cinématique opposée — raccourcissement ESE–WNW à SE–NW — vient se superposer à la schistosité 1 et l'oblitérer partiellement. Des réouvertures de la schistosité 1 interviennent au cours de ce second épisode. a) Carte de localisation des veines étudiées, b) Pillune – veta 14, c) Los Desemparados, d) Ticlla, e) veta Patricia, f) Mina Paula, g) Tocracancha – veta Plata, h) Sando Alcalde – veta 74 et i) veta Nazareño.

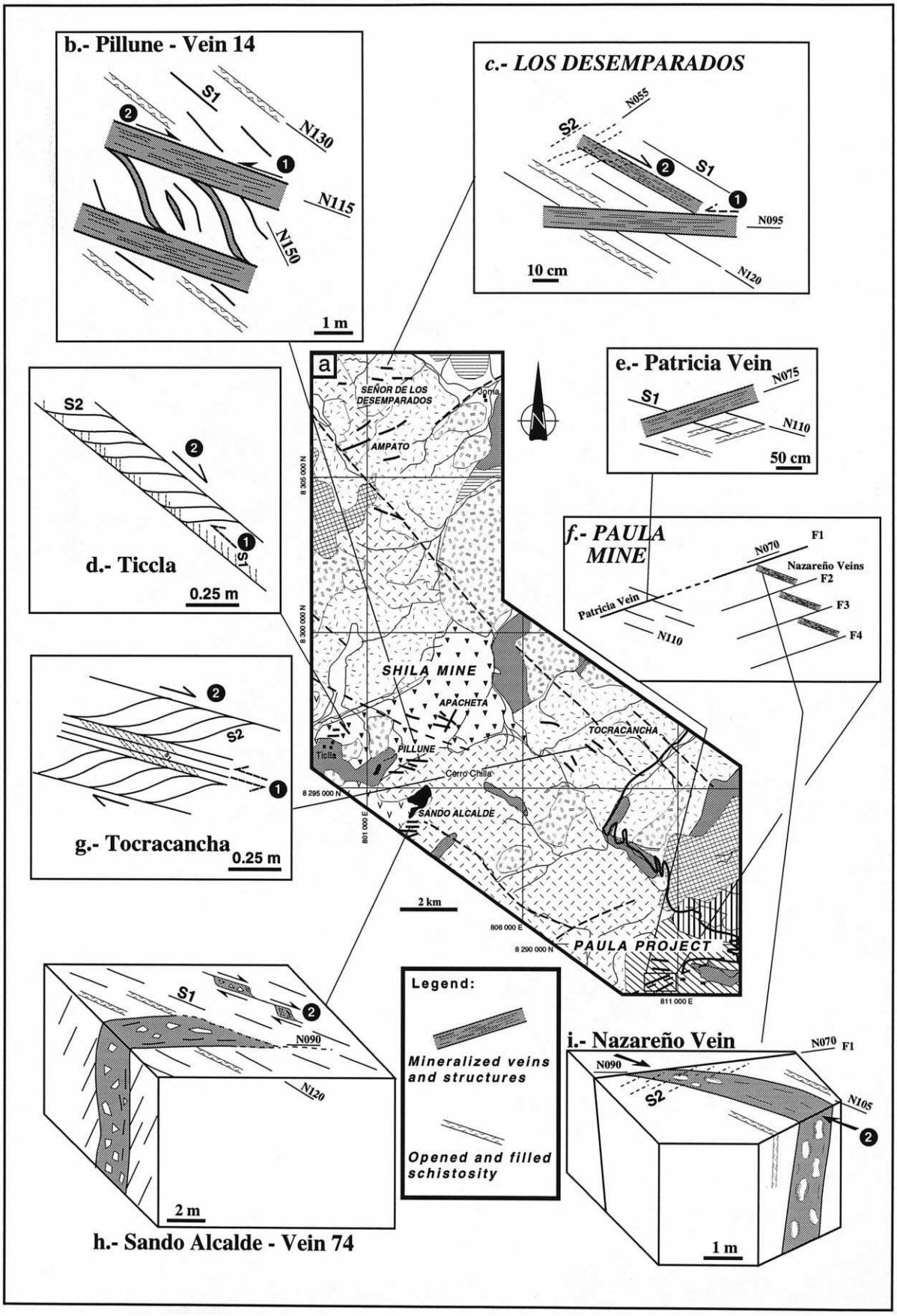
b.- Pillune - Vein 14
S1
N130
N115
N150
1 m
c.- LOS DESEMPARADOS
N055
S2
S1
N095
N120
10 cm
e.- Patricia Vein
N075
S1
N110
50 cm
d.- Ticcla
S2
S1
0.25 m
f.- PAULA MINE
N070
F1
Nazareño Veins
F2
F3
F4
Patricia Vein
N110
g.- Tocracancha
S2
0.25 m
a
SEÑOR DE LOS DESEMPARADOS
Jorna
AMPATO
SHILA MINE
APACHETA
TOCRACANCHA
PILLUNE
Ticlla
Cerro Chilla
SANDO ALCALDE
PAULA PROJECT
2 km
8 305 000 N
8 300 000 N
8 295 000 N
8 290 000 N
801 000 E
806 000 E
811 000 E
Legend:
Mineralized veins and structures
Opened and filled schistosity
S1
N090
N120
2 m
h.- Sando Alcalde - Vein 74
i.- Nazareño Vein
N070
F1
N090
S2
N105
1 m

Although several exceptions to the above general model are observed, the corresponding veins display no difference with the others as far as mineralogy and isotopic compositions ($^{206}Pb/^{204}Pb$: 18.54 to 18.60 [11]) are concerned.

(*i*) In the Apacheta area, veta 2 (N150°E) shows a few barren secondary fractures; evidence of both sinistral (probably related to the second deformation event) and dextral movement is observed. Veta 22 (N040–060°E) is not associated with secondary fractures and only shows evidence of sinistral movement. The dextral movement of veta 2 and the sinistral movement of veta 22 are probably related to the first shortening event suggesting relatively important stress deviations, possibly related to old structural patterns in the basement. This would explain fairly well the existence of identical kinematics for structures with considerably different orientations (*figure 2*).

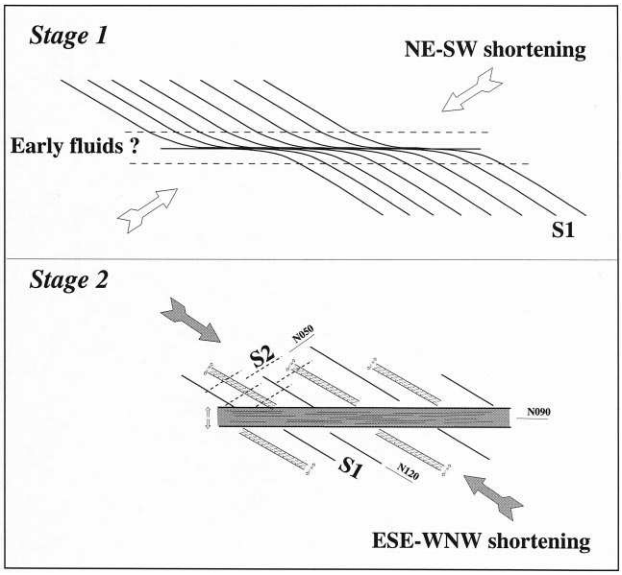

Figure 4. Mineralization formation model. Stage 1: creation of ≈east–west sinistral shear structures under NE–SW to ENE–WSW shortening conditions. Development of N120°E S1 schistosity. Possible emplacement of early hydrothermal fluids at the end of this stage. Stage 2: ESE–WNW to SE–NW shortening direction. Certain structures formed during stage 1 undergo dextral reactivation. The S1 schistosity is reopened by traction and/or shearing. S2 schistosity develops locally. Fracturing is assisted by hydrothermal fluids.

Figure 4. Modèle de formation des minéralisations. Stade 1 : création de structures décrochantes majoritairement est–ouest sous l'effet d'un raccourcissement orienté NE–SW à ENE–WSW. Développement d'une schistosité S1 orientée N120°E. Mise en place possible des premiers fluides hydrothermaux dès la fin de ce stade. Stade 2 : la direction de raccourcissement est orientée ESE–WNW à SE–NW. Certaines des structures apparues au stade 1 rejouent en dextre. La schistosité S1 est ré-ouverte, par tension et/ou cisaillement. Localement, une schistosité S2 se développe. Le processus de fracturation est assisté par les fluides hydrothermaux.

(*ii*) In the Mina Paula area, the Nazareño veta (N105°E) is intersected and offset by a group of approximately east–west-trending faults (F1 to F4; *figure 3f*). No clear evidence of strike-slip deformation is noted on the walls of this thick brecciated structure, which seems instead to have resulted from opening (or reopening) under stress during the second deformation event (*figure 3i*).

6. Discussion and conclusions

6.1. Mode of mineralization emplacement

The mineralization structures in the Shila-Paula area are interpreted as resulting from a reopening of the shear zones created during an earlier deformation event (*figure 4*). Stage 1 consists in formation of the ≈east–west sinistral shear zones under a NE–SW to ENE–WSW shortening direction, associated with the development of a S1 schistosity striking N120°E. During stage 2, these structures were reopened and channelled mineralizing fluids, the circulation of which may have begun during stage 1. This assumption is based on the fact that the textures of the main vein drastically differ from those of the secondary ones partly as the result of the stress rotation between stage 1 and 2. Reopening probably results from the combined action of tectonic stress (as evidenced by the local presence of S2 schistosity) and a high fluid pressure (fluid-assisted fracturing; e.g., [6]). The main veins are located along the ancient shear zones whereas the secondary fractures result from opening along the earlier S1 schistosity.

This mechanism accounts for most structures in the Shila-Paula mining district, despite certain specific zones (notably Apacheta) being difficult to integrate into this global framework (see above), and suggests a rotation of the shortening direction, the causes of which are still unknown.

6.2. Relation with the general geodynamic context

By comparing the radiometric data obtained for the Orcopampa–Arequipa area (*tables I– III*) with recent geological syntheses (e.g., [15]), it appears that mineralizing events are coeval with the major deformation phases, i.e., 17–15 Ma (Quechua I), 12–10 Ma (Quechua II) and 7–6 Ma (Quechua III) (e.g., [19, 20]). In addition, these data suggest that hydrothermal activity may have occurred 0–2 Ma after the volcanic activity with which it is associated [5].

The ENE–WSW to NE–SW shortening direction reconstructed for the first deformation event is consistent with paleo-stress field estimations for the considered area and period (Quechua II [8, 9, 12, 22]) and with the direction of convergence between the Nazca and South American plates [16, 18]. However, the second deformation event with an ESE–WNW to SE–NW shortening direction has not been described until now. This event

controlled mineralization emplacement in the Shila-Paula district and thus can be dated at about 10 Ma. The regional extent of this deformation event is at present unknown.

Version abrégée

1. Contexte géologique

Les veines épithermales de type adulaire–séricite de Shila–Paula sont situées dans la Cordillère occidentale, au nord-ouest d'Arequipa. Elles sont encaissées dans des brèches et des laves d'âge Miocène inférieur à moyen. 436 065 tonnes de minerai à 10,2 $g \cdot t^{-1}$ Au et 265,3 $g \cdot t^{-1}$ Ag ont déjà été produites. Les veines minéralisées ou 'vetas' sont en général peu puissantes (0,2 à 2,5 m), d'extension horizontale hectométrique et excèdent rarement 150 m de profondeur. Elles sont généralement orientées est–ouest (Pillune, Sando Alcalde, Ticala, Puncuhuayco, Mina Paula) ou NW–SE (Apacheta, Colpa, Tocracancha) et plus rarement NE–SW (Apacheta, Puncuhuayco, Ampato) (*figure 1*). Les pendages sont forts (> 75°), vers le nord ou vers le sud. Cette étude a pour but de préciser le contexte structural de mise en place de ces minéralisations, les travaux antérieurs étant peu nombreux et peu compatibles (e.g. [1, 3, 4, 10]).

2. Altération/minéralisation

La gangue des minéralisations est à quartz–rhodonite/rhodochrosite–adulaire. La paragenèse sulfurée est dominée par les sulfures et sulfosels d'argent, associés à pyrite–sphalérite–chalcopyrite–galène. L'électrum se dépose de façon synchrone à postérieure aux sulfures et sulfosels d'argent. L'altération hydrothermale des roches encaissantes est caractérisée par *i*) une potassification de la mésostase, *ii*) une pseudomorphose des phénocristaux de biotite et amphibole par un assemblage à chlorite–épidote–calcite, associé à une séricitisation des plagioclases magmatiques et des cristaux d'adulaire.

3. Datation

Les dacites non altérées, hôtes des vetas du secteur de Pillune, ont été datées (K/Ar, analyse en roche totale) à 13,0 ± 0,6 et 12,9 ± 0,6 Ma (*tableau I*) [13]. Des âges K/Ar de 10,94 ± 0,13 et 10,56 ± 0,12 Ma, ont été obtenus sur des cristaux d'adulaire provenant respectivement de Sando Alcalde et de Pillune (*tableau II*).

4. Contexte structural

Les décrochements contrôlant les minéralisations (*figure 2*) se répartissent en : (*i*) une population à cinématique décrochante senestre, orientée NE–SW à SE–NW et (*ii*) une population à cinématique décrochante dextre, orientée est–ouest à SSE–NNW. Le recouvrement entre les deux populations indique l'existence de plusieurs épisodes de déformation.

La majorité des structures minéralisées sont caractérisées par l'association entre une veine principale orientée N080°–N110°E et des fractures satellites orientées N120°–N135°E (*figure 3*). Cette géométrie est interprétée comme le résultat de la superposition de deux épisodes de déformation. Le premier se caractérise par des mouvements senestres sur des plans de cisaillements principaux orientés N080°–N110°E, associés à une schistosité de fracture S1 (orientée N120°–N135°E ; *figure 3*). Le second événement, à jeu dextre, lié à une direction de raccourcissement ESE–WNW à SE–NW, réactive ces deux types de structures et génère localement une schistosité S2, toujours sécante sur S1. Quelques vetas d'orientation différente (vetas 2 et 22, secteur d'Apacheta ; veta Nazareño, secteur de Mina Paula) s'éloignent de ce schéma général (*figure 3*).

5. Discussion. Conclusions

5.1. Modalité de mise en place des minéralisations

Un modèle de mise en place en deux stades, expliquant la majorité des structures minéralisées du district de Shila–Paula est proposé (*figure 4*). Le stade 1 correspond à la formation des zones de cisaillement sensiblement est–ouest décrochantes senestres sous les effets d'une direction de raccourcissement NE–SW à ENE–WSW, associées à une schistosité S1 N120°E. Dans un second stade, ces structures sont réouvertes et servent de réceptacle aux fluides minéralisateurs, dont la circulation a pu débuter dès la fin du stade 1. Ces réouvertures résultent vraisemblablement de l'action conjuguée d'une contrainte tectonique (présence locale d'une schistosité S2) et d'une pression élevée de fluides (fracturation assistée, e.g. [6]). Les filons principaux sont localisés le long des anciennes zones de cisaillement, alors que les fractures secondaires matérialisent les directions de l'ancienne schistosité S1.

5.2. Relation avec le contexte géodynamique général

La direction de raccourcissement ENE–WSW à NE–SW estimée pour le premier épisode de déformation est conforme aux estimations du champ des paléocontraintes pour la zone et la période considérée (phase tectonique Quechua II, autour de 12–10 Ma [8, 9, 12, 22]) et à la direction de convergence des plaques Nazca et Amérique du Sud [16, 18]. Le second épisode de déformation, avec une direction de raccourcissement ESE–WNW à SE–NW, n'a jamais été décrit auparavant.

Acknowledgements. This study (BRGM contribution N° 99030) was carried out as part of the PRD 406 development project entitled 'Metallogeny of the Andes' financed by the BRGM Research Division and as part of work on the 'Gold Theme' by the Metallogenic research group (GDR Métallogénie). The authors would like to thank Jean-Marie Georgel and CEDIMIN S.A. for their friendly assistance and logistical support as well as the geologists and engineers at Mina Shila and Mina Paula, particularly Uberto Ruiz and Carlos Velasquez. The text was translated by Rowena Stead of the BRGM Translation Department.

References

[1] Blès J.-L., Contexte structural des minéralisations aurifères épithermales d'Orcopampa, Layo et Shila (Département d'Arequipa, Pérou), BRGM Report 89 PER 054 GEO, 1989, 61 p. (unpublished).

[2] Candiotti de Los Rios H., Noble D.C., Mckee E.H., Geologic setting and epithermal silver veins of the Arcata district, Southern Peru, Econ. Geol. 85 (1990) 1473–1490.

[3] Fletcher C.N.J., Hawkins M.P., Trejada R., Structural control and genesis of polymetallic deposits in the Altiplano and Western Cordillera of southern Peru, J. South American Earth Sciences 2 (1989) 61–71.

[4] Fornari M., Vilca Neyra C., Mineralizacion argentifera asociada al volcanismo cenozoico en la faja Puquio-Cailloma, Boletin de la Sociedad Geológica del Perú 60 (1979) 101–128.

[5] Gibson P.C., McKee E.H., Noble D.C., Swanson K.E., Timing and interrelation of magmatic, tectonic, and hydrothermal activity at the Orcopampa district, Southern Peru, Econ. Geol. 90 (1995) 2317–2325.

[6] Gratier J.P., La déformation des roches par dissolution–cristallisation. Aspects naturels et expérimentaux de ce fluage avec transfert de matière dans la croûte supérieure, thesis, IRIGM, université de Grenoble, 1984, 315 p. (unpubl.).

[7] Heald P., Foley N.K., Hayba D.O., Comparative anatomy of volcanic-hosted epithermal deposits: acid-sulfate and adularia types, Econ. Geol. 82 (1987) 1–26.

[8] Huaman Rodrigo D., Évolution tectonique cénozoïque et néotectonique du Piémont pacifique dans la région d'Arequipa (Andes du Sud-Pérou), thesis, université Paris-Sud, Orsay, 1985, 220 p. (unpublished).

[9] Jaimes F., Romera D., Carlotto V., Marocco R., Cardenas J., La tectonica y la evolution geodinamica de la cuenca Paruro (Mioceno superior) en la región de Cusco, in: IX Congreso Peruano de Geología, Lima, Resúmenes Extendidos, Sociedad Geológica del Perú, vol. Esp. 1, 1997, pp. 337–340.

[10] Machare O.J., Ortega T.H., Estudio estructural del sector este de la veta Calera, Mina Orcopampa – Perú, in: IX Congresso Peruano de Geología – Lima, Resúmenes Extendidos, Sociedad Geológica del Perú, vol. Esp. 1, 1997, pp. 95–99.

[11] Marcoux E., Cassard D., Faure M., Llosa F., Andre A.S., Leroy J., Formación y evolución de las vetas epitermales Au–Ag en la Cordillera Shila, al sur del Perú, in: Comité Aurífero (Ed.), Third International Gold Symposium, Lima, 5–8 May 1998, Conferences Vol., pp. 392–399.

[12] Martinez C., Structure et évolution de la chaîne hercynienne et de la chaîne andine dans le Nord de la cordillère des Andes de Bolivie, Trav. Orstom 19, 1980, 352 p.

[13] Milesi J.-P., Marcoux E., Mineralogical and textural position of the Au–Ag bearing minerals in the evolution of epithermal deposits of Orcopampa and Shila (southern Peru), 1990 (unpublished report).

[14] Moncayo O.P., Estratigrafia, in: Geología del Peru, Boletin N° 55, Serie A, Carta Geologica Nacional, Ingemmet, 1995, pp. 45–86.

[15] Noble D.C., McKee E.H., The Miocene metallogenic belt of central and northern Peru, in: IX Congreso Peruano de Geología, Lima, Resúmenes Extendidos, Sociedad Geológica del Perú, vol. Esp. 1, 1997, pp. 115–119.

[16] Pardo-Casas F., Molnar P., Relative motion of the Nazca (Farallon) and South American plates since Late Cretaceous time, Tectonics 6 (1987) 233–248.

[17] Peterson P.S., Noble D.C., McKee E.H., Eyzaguirre V.R., A resurgent, mineralized caldera in Southern Peru: preliminary report, EOS Trans. American Geophys. Union 64 (1983) 884.

[18] Pilger R.H., Cenozoic plate kinematics, subduction and magmatism: South American Andes, J. Geol. Soc. London 141 (1984) 793–802.

[19] Sébrier M., Soler P., Tectonics and magmatism in the Peruvian Andes from Late Oligocene times to Present, in: Harmon R.S., Rapela C.W. (Eds.), Andean Magmatism and its Tectonic Setting, Geol. Soc. Am., Spec. Pap. 265 (1991) 259–278.

[20] Sébrier M., Lavenu A., Fornari M., Soulas J.-P., Tectonics and uplift in Central Andes (Peru, Bolivia and Northern Chile) from Eocene to Present, Géodynamique 3 (1988) 85–106.

[21] Silberman M.L., McKee E.H., Noble D.C., Age of mineralization at the Cailloma and Orcopampa silver districts, Southern Peru, Isochron/West 43 (1985) 17–18.

[22] Soulas J.-P., Les phases tectoniques andines du Tertiaire supérieur, résultats d'une transversale Pisco–Ayacucho (Pérou central), C. R. Acad. Sci. Paris, série D 284 (1977) 2207–2210.

[23] Vidal J.-C., Geología de los cuadrangulos de Huambo y Orcopampa, Boletin N° 46, Serie A, Carta Geológica Nacional, Ingemmet, 1993, 62 p.